

## **AN INVESTIGATION ON THE EFFECT OF FUNCTIONALISED GRAPHENE COMPOSITED WITH NCNT AND FE-NCNT ON THE OXYGEN REDUCTION REACTION VIA PHYSICAL MIXING METHOD**

CHONG W.Z., WONG W.Y.\* , RASHMI WALVAKER

School of Engineering, Taylor's University, Taylor's Lakeside Campus,  
No. 1 Jalan Taylor's, 47500, Subang Jaya, Selangor DE, Malaysia  
\*Corresponding Author: WaiYin.Wong@taylors.edu.my

### **Abstract**

Oxygen reduction reaction plays a major role in fuel cell applications to generate electricity by an electrochemical reaction. In this study, functionalised graphene composited with Fe-NCNT or NCNT were investigated on its ORR activity using a physical mixing method. Initially, functionalised graphene was produced via oxidation of graphene. NCNT and Fe-NCNT was obtained from the previously prepared samples using chemical vapour deposition technique and electrochemical reduction method for Fe-NCNT. The physical mixing between functionalised graphene and NCNT or Fe-NCNT was performed using sonication with the presence of pyrrole to produce the desired nanocatalyst. The surface morphologies and microstructures of the synthesised nanocatalysts were studied using field emission scanning electron microscopy. Surface chemical functionality of the nanocatalysts was investigated using X-ray photoelectron microscopy. Meanwhile, the ORR performance of nanocatalysts in a half cell were investigated using cyclic voltammetry techniques in both alkaline and acidic electrolytes. From this study, agglomeration of functionalised graphene (f-graphene) was observed on the Fe-NCNTs indicating a hindrance in transfer of electrons within the catalyst surface. NCNT/f-graphene showed to contain higher percentage of pyridinic-N which claimed to have favored the catalytic activity compared to Fe-NCNT/f-graphene. Likewise, a higher onset potential was recorded for NCNT/f-graphene which indicated a higher ORR activity than the Fe-NCNT/f-graphene.

Keywords: Oxygen reduction reaction, Nanocatalyst, Functionalised graphene, Nitrogen-doped carbon nanotubes, Fuel cell.

### **1. Introduction**

Fuel cell reaction involves a catalyst-facilitated electrochemical reaction between oxygen and hydrogen to form water along with the generation of electricity [1].

Fuel cell is similar to battery in that it generates electricity from an electrochemical reaction and as a byproduct, heat energy is released [2]. However, a battery store limited amount of energy within it and once it is depleted, the battery must be discarded, or recharged by using an external supply of electricity to drive the electrochemical reaction in the reverse direction. On the other hand, a fuel cell uses external supply of energy (fuel) to go indefinitely, as long as it is supplied with a source of hydrogen and a source of oxygen (usually air). In today's fuel cell, platinum is the most commonly used catalyst in electrodes for fuel cells due to its high catalytic activity [3]. However, using platinum as the catalyst has a drawback due to the cost consuming of its metal components. Thus, commercialising it has always been a thought in many minds from practical point of view. In recent studies [4], a group of researchers have developed an inexpensive graphene-based fuel cell catalyst that was claimed to perform better than a commercial platinum equivalent in oxygen reduction reaction (ORR) as well as tolerating both carbon monoxide poisoning, a common issue for fuel cell stacks, and methanol crossover. Nitrogen-doped carbon nanotubes (NCNT) have been explored as the metal-free catalysts that also showed to exhibit appreciable ORR activities in fuel cells [5].

In this context, graphene is consider as the suitable candidate to mix with ORR active NCNT to act as the catalyst to enhance the ORR activity because it can be easily synthesised by using the modified Hummer's method [6]. The graphene structure which composed of a single layer of graphitic carbon [7] possesses the property that can be readily chemically functionalised [8-9]. Besides, functionalisation of graphene such as nitrogen doping can demonstrate the ability for catalysing the ORR due to their unique electronic properties derived from the conjugation between the nitrogen lone-pair electrons and the graphene  $\pi$  system [10]. On the other hand, through the studies of Wong et al. [11], it was demonstrated that the NCNT with highest ratio of pyridinic-N/quaternary-N was shown to exhibit higher ORR activity in both alkaline and acidic media. In this case, the pyridinic- N edge would most likely be the key on the influence of ORR activity.

When extra electrons are introduced into the graphite network through doping, the electron donation process from carbon to oxygen can be facilitated which also leads to the enhanced ORR activity. The enhanced ORR activity can be explained by the modification of electronic structure of carbon by nitrogen which increases the edge plane exposure by creating defects on carbon. This can be done due to the incorporation of nitrogen atom in the matrix of carbon can withdraw electrons from carbon because of the higher electronegativity of nitrogen. From a study [12], Fe-NCNT which has shown to have higher catalytic activity in ORR compared to NCNT will be used in this study. Catalytic activity determined from CV analysis shows that Fe-NCNT has a higher value of offset potential, above 0.6 V, compared to NCNT with 0.58 V. Current peak for Fe-NCNTs also shift to more positive which is at 0.4 V compared to 0.3 V for NCNT. Therefore, the objectives of this research are to synthesis nanocatalysts of Fe-NCNT/f-graphene and NCNT/f-graphene using physical mixing method and to investigate the effect of compositing f-graphene on the surface morphology, surface chemical functional groups and oxygen reduction activity of the nanocatalysts. The reason of selecting physical mixing in this study is due to the fact that, the presence of opposite charges on NCNT and f-graphene is believe to be physical adsorbed in

the sense that functionalised NCNT provides an electron induced surface with both partial positive and negative charges [13] while the f-graphene produced from the oxidation of graphene provides -COOH carboxylic group and -OH hydroxyl group [14] which are hypothetically achievable through physical mixing. In this case, a fundamental study on the ORR for Fe-NCNT/f-graphene and NCNT/f-graphene using physical mixing method was studied before the method can be fine-tuned to improve the catalytic activity of the sample in order to determine whether they offer improved performance relative to that without f-graphene composite.

## **2. Experimental**

### **2.1. Synthesis of f-graphene**

Oxidation method or carboxylation was used to synthesis functionalised graphene from graphene [15]. 1.2 g of graphene was added to 30 ml H<sub>2</sub>SO<sub>4</sub> and 10 ml of HNO<sub>3</sub> (3:1 v/v). The mixture was allowed to mix vigorously using Soxhlet equipment for 7 hours at 70 °C for oxidation to take place. Washing process were carried out using simple decantation of supernatant via a centrifugation technique with a centrifugation force of 8000 rpm for 15 mins (MEGAFUGE 40R) (mega centrifuge; 50ml falcon tubes). The product was washed repeatedly with deionised water until a pH 7 is achieved. Lastly, the sample was collected and dried at 60°C for 1 day.

### **2.2. Synthesis of NCNT and Fe-NCNT**

NCNT was prepared via chemical vapour deposition (CVD) technique using iron (II) phthalocyanine as precursor and ethylenediamine as carbon and nitrogen source as described in previous paper [16]. Fe-NCNT was prepared by chemical impregnation with iron (III) nitrate nanohydrate (FeN<sub>3</sub>O<sub>9</sub>.9H<sub>2</sub>O) and chemical reduction at 500 °C for 4 hours under nitrogen flow condition [12].

### **2.3. Preparation of Fe-NCNT/f-graphene and NCNT/f-graphene nanocatalysts**

Initially, 10 mg of 5% Fe-NCNT was mixed with f-graphene with the ratio of 1:1 at normal condition. Then, 100 mg of was dissolved into the Fe-NCNT/f-graphene suspension above at the weight ratio of 1:10 (Fe-NCNT: pyrrole) while the mixture was diluted using 10mL of water. The resulted mixture was homogenised with the aid of ultrasonication for 2 hours. During sonication, oxidative polymerisation of pyrrole occurs and was expected to assist in the formation of the nanocomposite between nanotubes and f-graphene. A second sample of 5% Fe-NCNT mixed with f-graphene was prepared at the ratio of 1:0 using the same procedures above. The experiment was repeated with the same volume ratio of pure NCNT. The final obtained catalyst was labelled as 5% Fe-NCNT/GO (1:1), 5% Fe-NCNT/GO (1:0), NCNT/GO (1:1) and NCNT/GO (1:0) based on the volume ratio.

## 2.4. Physicochemical characterisation

The surface morphologies of the 5% Fe-NCNT/f-graphene ratio 1:1 and NCNT/f-graphene ratio 1:1 samples were characterised by field emission scanning electron microscopy (FESEM) on Hitachi SU8030 microscope operated at 2 kV. For FESEM analysis, the samples were loaded evenly on the sample holder before entering the scope chamber. The samples were checked to ensure all samples fit under the gauge and no part of it is touching or taller than the gauge. The nitrogen contents of the surfaces of all samples were determined by X-ray photo electron spectroscopy (XPS) on PHI Quantera II instrument operated at 14kV. The XPS analysis was conducted using a dual-anode X-ray source with Al K-alpha irradiation with energy of 1486.8 eV. A survey scan was performed from 1200 to 16 eV on 5% Fe-NCNT/f-graphene ratio 1:1 and NCNT/f-graphene ratio 1:1 samples, followed by a narrow scan specifically on the C 1s, N 1s, O 1s and Fe 2p regions for 5% Fe-NCNT/f-graphene ratio 1:1 while C 1s, N 1s and O 1s regions for NCNT/f-graphene ratio 1:1. The obtained data were analysed using a compatible software with the XPS data.

## 2.5. Electrochemical characterisation

The electrocatalytic activity of the Fe-NCNT/f-graphene samples was measured on an Autolab PGSTAT128N potentiostat using the cyclic voltammetry technique in a standard three-electrode cell with 5 mm diameter glassy carbon (GC) served as the working electrode, platinum wire served as the auxiliary electrode, and Ag/AgCl was used as the reference electrode. The analysis was done in 2 conditions by utilising electrolyte of either a N<sub>2</sub>- or O<sub>2</sub>-saturated 0.5 M H<sub>2</sub>SO<sub>4</sub> solution and 0.1 M KOH. The catalyst ink that contained of 0.2 mL Fe-NCNTs/f-graphene mixed with 0.5mL of 10wt% Nafion solution was prepared by ultrasonication. 15  $\mu$ L of the catalyst ink was deposited evenly on the GC electrode surface and was subsequently dried at room temperature careful to prevent contamination on the catalyst ink. The electrode was visually inspected to ensure a uniform film formation and that no catalyst ink was contacting the ring portion of the electrode. Prior to the electrochemical measurements, the as-prepared sample electrode was rinsed with deionised water before being placed into the electrochemical cell. The potential window was set at 1.0 V to -0.4 V in the negative scan mode. Each scan was repeated 3 times to obtain a stable cyclic voltammogram.

## 3. Results and Discussions

### 3.1. Physical characterisation (FESEM)

Field emission scanning electron microscopy (FESEM) was used to perform the physical characterisation of the samples synthesised in order to study the structural morphology of the samples. The surface morphologies of the Fe-NCNT/f-graphene as shown in Fig. 1(a) clearly observed that the iron particles were deposited carbon nanotube. Graphene flakes were found to be mixed with Fe-NCNT in a random manner. During physical adsorption of Fe-NCNT on the graphene surface, the iron nanoparticles were not able to bind onto the thin-layer graphene sheet. This resulted in a crooked surface of the nanotube that was partially detached from the graphene layers. As observed from Fig. 1(a), the GO

tends to form very dense agglomerates with layered structure around the carbon nanotubes due to the van der Waals interaction between the graphene layers [17]. Agglomeration in such manner has formed a barrier in the active sites, hindering the ORR activity of the nanocomposites.

Similarly, the NCNT/f-graphene displayed in Fig. 1(b) demonstrated a surface morphology of agglomeration in graphene sheets that forms blockage on the active sites which inhibit the ORR mechanism on the nanocomposite. Agglomeration of graphene sheets presence in the Fe-NCNT/f-graphene and NCNT/f-graphene would in turn leads to the ineffective electron transfer within the catalyst surface. Nonetheless, the absence of iron nanoparticles deposited on NCNT/f-graphene sample has demonstrated a smoother graphitic structure on the carbon nanotubes. As compared to both the Fe-NCNT/f-graphene and NCNT/f-graphene surface morphologies, pure NCNT has displayed a less corrugated structure as reported in previous study [18].

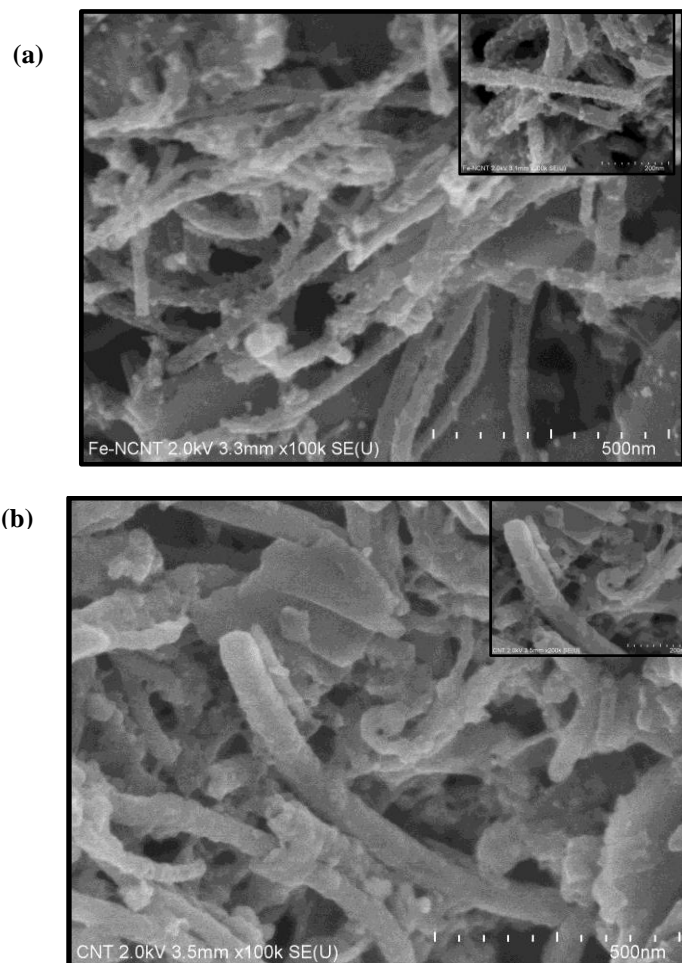


**Fig. 1. FESEM images of (a) 5% Fe-NCNT/rGO (b) NCNT/rGO and (c) NCNT at magnification of 100,000 times. Inset shows at magnification of 200,000 times.**

### 3.2. X-ray photoelectron spectroscopy

To investigate on the surface composition and the chemical states of the nitrogen atoms of the synthesised Fe-NCNTs/f-graphene samples, XPS studies was done by determining the nitrogen content in the samples. From the survey scan on the XPS spectrum as presented in Table 1, the nitrogen content can be seen to have relatively high concentration in both 5% Fe-NCNT/f-graphene and NCNT/f-graphene (11.67 at.% and 14.31 at.% respectively). Although the two samples may seem closely similar in terms of carbon concentration and oxygen concentration, there is the presence of iron particles in the Fe-NCNT/f-graphene sample which can be observed from Fig. 2 presented. XPS analysis shows trace amount of iron (0.76 at.%) in the Fe-NCNT/f-graphene sample. The presence of iron in the NCNT has displayed different nanotubes surface morphologies of the samples as shown previously in Fig. 1.

In order to further study the chemical bonding on the nanocatalyst synthesised, the N 1s region of both the Fe-NCNT/f-graphene and NCNT/f-graphene has to be deconvoluted to study the structural defects in the nitrogen configuration of the nanotubes formed. As demonstrated in Fig. 3, both nanocatalysts possess the nitrogen configuration of pyrrolic-N and pyridinic-N. As stated from previous study [18], the high concentration of surface defects presence in the pyridinic-N configuration at the nanotubes surface favoured the ORR catalytic activity. Therefore, in this research, the distinguishable surface defects of the pyridinic-N will be considered. The nitrogen configuration in N 1s region of both the samples are shown in Fig. 3, the pyridinic-N (binding energy  $398 \pm 0.2$  eV) and pyrrolic-N (binding energy  $400 \pm 0.2$  eV) are exhibited on Fe-NCNT/f-graphene while pyridinic-N (binding energy  $399 \pm 0.2$  eV) and pyrrolic-N (binding energy  $400 \pm 0.2$  eV) are exhibited on NCNT/f-graphene.

Comparing both Fe-NCNT/f-graphene and NCNT/f-graphene, having relatively similar nitrogen content, the NCNT/f-graphene showed a higher concentration of tube defects, which showed to contain a much higher percentage of pyridinic-N group. Pyridinic-N is implying that the nitrogen atoms bonded to the edge of the graphene planes with two adjacent carbon atoms; these atoms donate one p-electron to the aromatic  $\pi$  system [19] and have been claimed to be responsible for the high degree of defects that produces a rugged surface. To this, the detail analysis of the N 1s spectra has shown that the NCNT/f-graphene makes a more desirable nanocatalyst for ORR mechanism. The ORR activity with respect to the nitrogen groups could be explained by the theory regarding the edge plane nitrogen groups (pyrrolic or pyridinic) being the active site for ORR due to the lone pair electrons [20]. From this trend, as reported from previous study [18], at higher nitrogen content, the formation of pyridinic nitrogen group are more favourable due to low heat of formation [20] which are demonstrated in this research.

Moreover, the presence of -COOH and -OH groups due to the oxidation of graphene can be confirmed in Fig. 4 with the peak deconvoluted at 288.0 eV (C=O) and at 286.8 eV (C-O). In addition, the peak at 285.8 eV was attributed to the nitrogen atom that was doped into the carbon matrix of NCNT.

**Table 1. Atomic percentage of the samples and its N distribution from XPS spectra of the synthesised Fe-NCNT/f-graphene and NCNT/f-graphene samples.**

Samples	C content (at %)	O content (at %)	N content (at %)	Weight distribution of N (%)	
				Pyrolic N (%)	Pyridinic N (%)
5% Fe-NCNT/f-graphene	71.55	12.34	11.67	92.5	7.5
NCNT/f-graphene	63.69	20.14	14.31	30.67	69.33

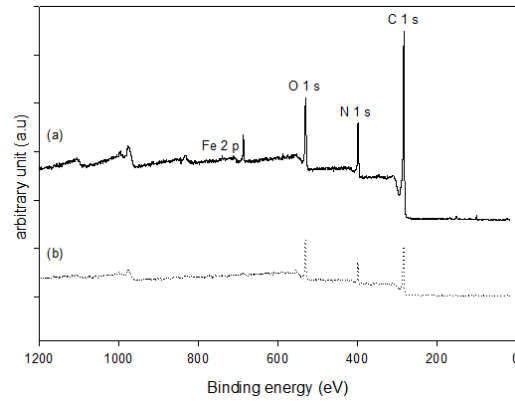


**Fig. 1. High resolution XPS analysis in survey scans for (a) 5% Fe-NCNT/f-graphene and (b) NCNT/f-graphene.**

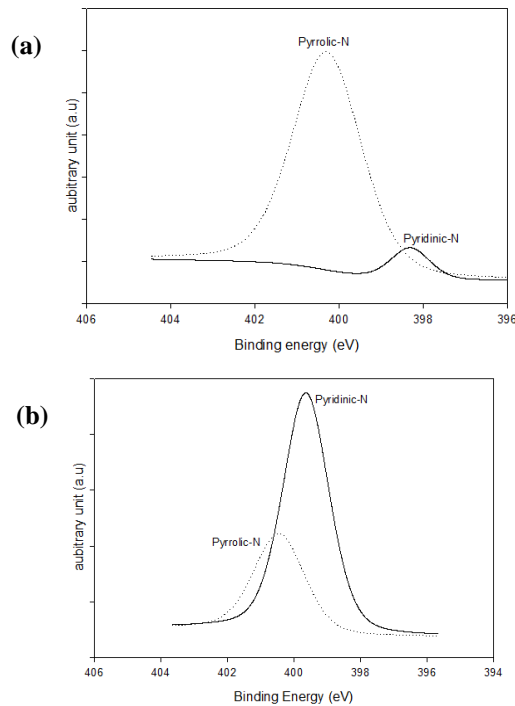


**Fig. 2. High resolution XPS analysis in N 1s region for (a) 5% Fe-NCNT/f-graphene and (b) NCNT/f-graphene nanocatalyst synthesised**

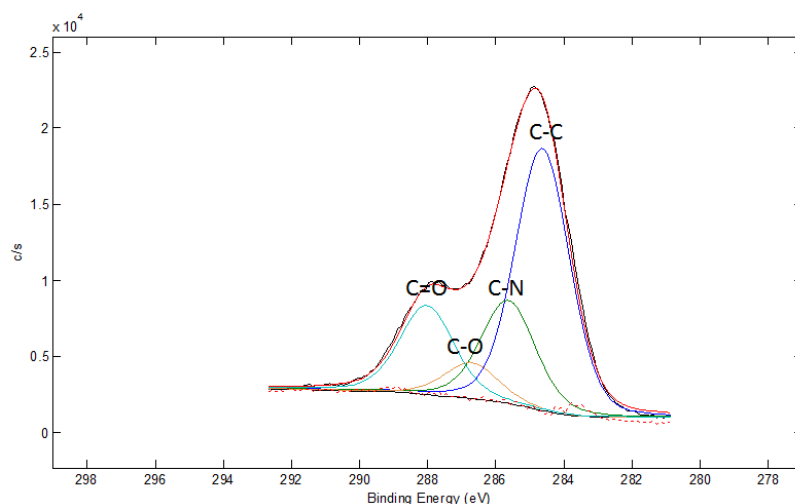


**Fig. 4. High XPS spectra in C 1s region measured on NCNT/f-graphene sample.**

### 3.3. Electrochemical analysis

Cyclic voltammetry (CV) was used to investigate the ORR catalytic activity of the Fe-NCNTs/f-graphene and NCNT/f-graphene synthesised. A qualitative analysis on the oxygen reduction ability of the nanocatalysts which can be determined from the onset potential and reduction peak potential in the voltammograms was performed. The CV test was conducted in two stages in which the samples are exposed in both alkaline media and acidic media to study the catalytic performance. A background scan was performed under the nitrogen-saturated environment as a control set before the voltammogram was recorded in oxygen-saturated environment. Initially, the CV analysis was started off with both Fe-NCNTs/f-graphene and NCNT/f-graphene nanocatalyst in alkaline media of 0.1 M KOH electrolyte, which the voltammograms recorded, is presented in Fig. 5. Previous study [18] has reported the catalytic activity of NCNTs in acidic media showing a potential window of - 0.4 V to + 1.0 V vs. Ag/AgCl, which will be incorporated into this research. The result has surprisingly exhibited that the 5% Fe-NCNT/f-graphene shown in Figs. 4(a) and (b) has a closely identical catalytic performance as displayed by NCNT/f-graphene shown in Figs. 4(c) and (d) with a peak -0.4 V (vs Ag/AgCl). This in turn, states that the incorporation of metal alloy on the NCNT has not made a significant impact on the catalytic performance on ORR mechanism possibly resulted from the blockage of active sites by the agglomerated functionalised graphene flakes.

At the second phase of the CV analysis, acid media of 0.5 M H<sub>2</sub>SO<sub>4</sub> electrolyte was used to investigate the significant difference compared to alkaline media while the samples are conducted in both N<sub>2</sub>- and O<sub>2</sub>-saturated environment as well. The voltammograms recorded are displayed in Fig. 5. As expected, the Fe-NCNTs/f-graphene as well as NCNT/f-graphene nanocatalyst has not shown any significant catalytic performance under acidic media. This occurrence can be related to the sluggish ORR kinetics of oxygen reduction process in acidic aqueous solution particularly on NCNT [21].



The inactive role of Fe metal in Fe-NCNT has also reflected on the lower onset potential (-0.3 V) in alkaline media as compared to that of NCNT (-0.2 V). On top of that, a variety of non-noble metals are known to be suitable candidate as active catalysts for ORR in alkaline media [22]. The relatively high positive onset potential in alkaline media and the high current density in that of the O<sub>2</sub>-saturated condition strongly agree that the NCNT was a more active catalyst for the ORR in alkaline media. Even so, with the agglomeration of graphene sheets on the NCNT as shown in Fig. 1, the effectiveness of electron transfer within the catalyst surface has deteriorated greatly due to the blockage of active sites on the nanocomposite.

To analyse the CVs result, this study will be focusing on the electrochemical activities in the alkaline media which shows appreciable performance. Referring to the CVs result shown in Figs. 4(a) and (b), the 5% Fe-NCNT/f-graphene (1:0) demonstrated a significant peak at -0.3 V(vs Ag/AgCl), while 5 % Fe-NCNT/f-graphene (1:1) exhibit an imperceptible peak at the similar peak as a possible result of agglomeration of graphene on the NCNT as presented in Fig. 1. This agglomeration behavior has severely disrupted the surface structural characteristic of the NCNT which reflected on the low degree of surface defects that is highly crucial to ORR activity by exposing more edge plane nitrogen groups such as pyridinic and pyrrolic nitrogen which could participate in the ORR through the lone pair electrons [21]. Similar trend was observed in the NCNT/f-graphene (1:1) and NCNT/f-graphene (1:0) presented in Figs. 4(c) and (d) that does not have Fe deposition. Due to the fact that stable dispersion was not able to be established during mixing process, it resulted in graphene sheet agglomerated on the NCNT and thus, inhibited the ORR activity on the nanocomposite. Furthermore, physical mixing was incorporated in this study which possibly leads to the existence of van der Waals forces in the graphene sheets during the dispersion process. For further studies, chemical mixing such as hydrothermal treatment [23] could be an alternative choice in order to break the bonds between the graphene sheets, thus establish a stable reaction between NCNT and graphene.

According to Figs. 4(a) and (c), it can be seen that the NCNT/f-graphene (1:1) has a higher onset potential of -0.2 V(vs Ag/AgCl) in comparison to that of the 5 % Fe-NCNT/f-graphene (1:1) at -0.3 V(vs Ag/AgCl). This unforeseen behavior may be due to the lack of efficiency of iron in acting as the active sites for ORR and to further deteriorate it, the number of active sites on NCNT was block due to the Fe deposition. In addition, the expected redox peaks were not displayed in the positive potential range of the voltammogram, suggesting that the iron particles did not play a role in ORR in Fe-NCNT/f-graphene sample.

From this study, it was shown that the f-graphene in the Fe-NCNT/f-graphene and NCNT/f-graphene nanocatalysts synthesised via physical mixing does not seem to enhance the catalytic activity towards oxygen reduction comparable to NCNT catalyst. The shortcoming of f-graphene on the improvement on ORR activity most probably caused by the fact, that physical mixing is not a suitable method for the compositing process.

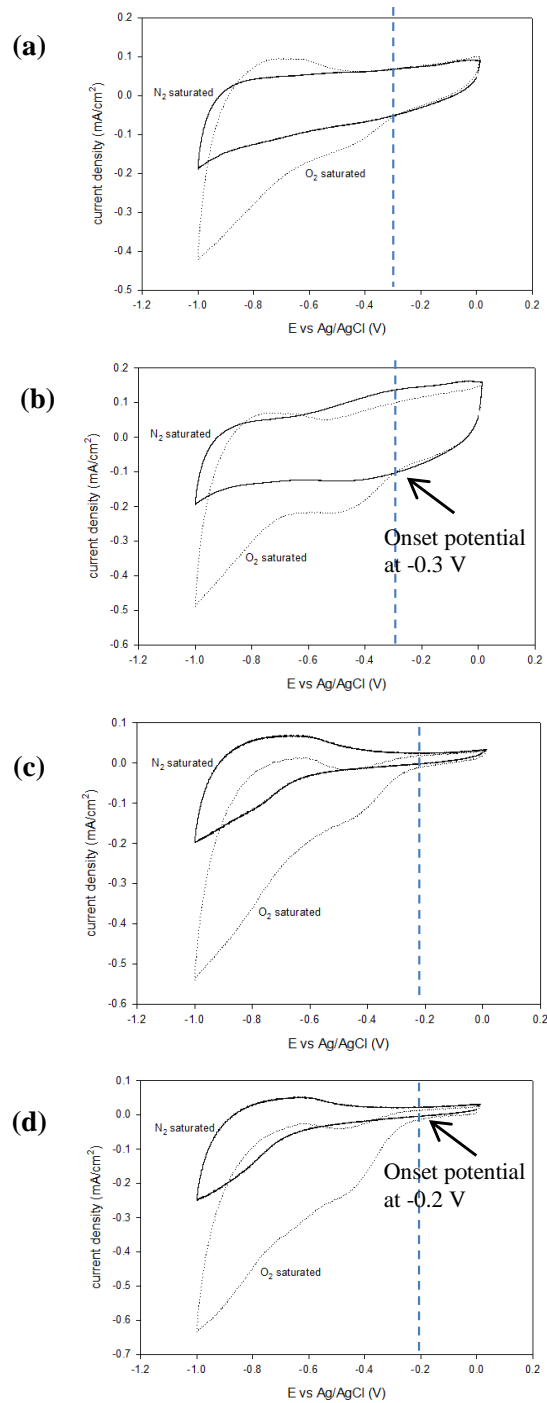


**Fig. 5. Cyclic voltammogram of (a) 5%Fe-NCNT/f-graphene (1:1) (b) 5%Fe-NCNT/f-graphene (1:0) (c) NCNT/f-graphene(1:1) (d) NCNT/f-graphene(1:0) GC electrode in  $N_2$ -saturated and  $O_2$ -saturated 0.1 M KOH electrolyte. Potential scan rate at 5 mV/s.**

#### 4. Conclusions

Fe-NCNT/f-graphene and NCNT/f-graphene nanocatalysts were synthesised using physical mixing method by ultrasonication with the presence of pyrrole. Through the physical characterisation, it appears that the graphene sheet forms agglomerates on the NCNT and thus, inhibit the ORR activity on the nanocomposite, through the blockage of the active sites. In conjunction, agglomeration of graphene also results in the ineffective electron transfer within the catalyst surface. In electrochemical wise, the functionalised graphene synthesised has not shown significant improvement in ORR activity. The most probable factor leading to this deficiency is due to the compositing process which utilises physical mixing instead of chemical mixing. Likewise, from this study, the iron particles might not be effective in acting as active sites for ORR that was observed from the result that NCNT/f-graphene has shown superior electrochemical properties in comparison to Fe-NCNTs/f-graphene synthesised. Therefore, as a conclusion, NCNT/f-graphene is considered a more suitable candidate as per this study for ORR in fuel cell application.

#### Acknowledgment

This research work was financially supported by the research funds from School of Engineering, Taylor's University. The authors also gratefully acknowledged the support of the Fuel Cell Institute, University Kebangsaan Malaysia for materials and equipment usage.

#### References

1. Anon (2014). Fuel cell introduction - Fuel cell today. Retrieved October 2, 2014, from <http://www.fuelcelltoday.com/about-fuel-cells/introduction>.
2. Breeze, P. (2005). *Power generation technologies*. Elsevier.
3. Raso, M.A.; Carrillo, I.; Mora, E.; Navarro, E.; Garcia, M.A.; and Leo, T.J. (2014). Electrochemical study of platinum deposited by electron beam evaporation for application as fuel cell electrodes. *International Journal of Hydrogen Energy*, 39(10), 5301-5308.
4. Bai, J.; Zhu, Q.; Lv, Z.; Dong, H.; Yu, J.; and Dong, L. (2013). Nitrogen-doped graphene as catalysts and catalyst supports for oxygen reduction in both acidic and alkaline solutions. *International Journal of Hydrogen Energy*, 38(3), 1413-1418.
5. Li, H.; Liu, H.; Jong, Z.; Qu, W.; Geng, D.; Sun, X.; and Wang, H. (2011). Nitrogen-doped carbon nanotubes with high activity for oxygen reduction in alkaline media. *International Journal of Hydrogen Energy*, 6(3), 2258-2265.
6. Shahriary, L.; and Athawale, A.A. (2014). Graphene oxide synthesized by using modified hummers approach. *International Journal of Renewable Energy and Environmental Engineering*, 2(1), 58-63.
7. Chang, C.; Chang, K.; Shen, H.; and Hu, C. (2014). A unique two-step Hummers method for fabricating low-defect graphene oxide nanoribbons through exfoliating multiwalled carbon nanotubes. *Journal of the Taiwan Institute of Chemical Engineer*, 45(5), 2762-2769.

8. Elias, D.C.; Nair, R.R.; Mohiuddin, T.M.G.; Morozov, S.V.; Blake, P.; Halsall, M.P.; Ferrari, A.C.; Boukhvalov, D.W.; Katsnelson, M.I.; Geim, A.K.; and Novoselov, K.S. (2009). Control of graphene's properties by reversible hydrogenation: Evidence for graphane. *Science*, 323(5914), 610-613.
9. Loh, K.P.; Bao, Q.; Ang, P.K.; and Yang, J. (2010). The chemistry of graphene. *Journal of Materials Chemistry*, 20(12), 2277-2289.
10. Li, M.; Zhang, L.; Xu, Q.; Niu, J.; and Xia, Z. (2014). N-doped graphene as catalysts for oxygen reduction and oxygen evolution reactions: Theoretical considerations. *Journal of Catalysis*, 314, 66-72.
11. Wong, W.Y.; Daud, W.R.W.; Mohamad, A.B.; Kadhum, A.A.H.; Loh, K.S.; and Majlan, E.H. (2011). Density functional theory study of oxygen reduction mechanism at nitrogen-doped carbon nanotubes for fuel cell applications. *Advanced Materials Research*, 233-235, 17-22.
12. Fadzillah, D.M. (2013). *Synthesis and characterisation of composite metal with NCNT catalyst for PEM fuel cell application*. Thesis. Universiti Kebangsaan Malaysia, Selangor, Malaysia.
13. Balasubramanian K.; and Burghard, M. (2005). Chemically functionalized carbon nanotubes. *Small*, 1(2), 180-192.
14. Kuila, T.; Bose, S.; Mishra, A.K.; Khanra, P.; Kim, N.H.; and Lee, J.H. (2012). Chemical functionalization of graphene and its applications. *Progressive Materials Science*, 57(7), 1061-1105.
15. Chhabra, V.A.; Deep, A.; Kaur, R.; and Kumar, R. (2012). Functionalization of graphene using carboxylation process. *International Journal of Science and Emerging Technologies with Latest Trends*, 4(1), 13-19.
16. Wong, W.Y.; Daud, W.R.W.; Mohamad, A.B.; Kadhum, A.A.H.; Loh, K.S.; Majlan, E.H.; and Lim, K.L. (2014). The impact of loading and temperature on the oxygen reduction reaction at Nitrogen-doped carbon nanotubes in alkaline medium. *Electrochimica Acta*, 129, 47-54.
17. Yan, J.; Wei, T.; Shao, B.; Ma, F.; Fan, Z.; Zhang, M.; Zheng, C.; Shang, Y.; Qian, W.; and Wei, F. (2010). Electrochemical properties of graphene nanosheet/carbon black composites as electrodes for supercapacitors. *Carbon*, 48(6), 1731-1737.
18. Wong, W.Y.; Daud, W.R.W.; Mohamad, A.B.; Kadhum, A.A.H.; Loh, K.S.; and Majlan, E.H. (2013). Influence of nitrogen doping on carbon nanotubes towards the structure, composition and oxygen reduction reaction. *International Journal of Hydrogen Energy*, 38(22), 9421-9430.
19. Wang, C.; Huang, Z.; Zhan, L.; Wang, Y.; Qiao, W.; Liang, X.; and Ling, L. (2011). Nitrogen-doped carbon nanotubes synthesized with carbon nanotubes as catalyst. *Diamond and Related Materials*, 20(10), 1353-1356.
20. Chen, Z.; Higgins, D.; and Chen, Z. (2010). Nitrogen doped carbon nanotubes and their impact on the oxygen reduction reaction in fuel cells. *Carbon*, 48(11), 3057-3065.
21. Chen, Z.; Higgins, D.; and Chen, Z. (2010). Electrocatalytic activity of nitrogen doped carbon nanotubes with different morphologies for oxygen reduction reaction. *Electrochimica Acta*, 55(16), 4799-4804.

22. Ramaswamy, N.; and Mukerjee, S. (2012). Fundamental mechanistic understanding of electrocatalysis of oxygen reduction on Pt and non-Pt surfaces: Acid versus alkaline media. *Advances in Physical Chemistry*, 2012, Article ID 491604, 1-17.
23. You, B.; Wang, L.; Yao, L.; and Yang, J. (2013). Three dimensional N-doped graphene-CNT networks for supercapacitor. *Chemical Communications*, 49(44), 5016-5018.